Nuclear Instruments and Methods in Physics Research A 763 (2014) 177–183

Contents lists available at ScienceDirect

Nuclear Instruments and Methods in Physics Research A

journal homepage: www.elsevier.com/locate/nima

Monitoring reactions for the calibration of relativistic hadron beams

A. Ferrari [a], F.P. La Torre [a,b], G.P. Manessi [a,c,*], F. Pozzi [a,d], M. Silari [a]

[a] CERN, 1211 Geneva 23, Switzerland
[b] University of Bern, AEC-LHEP, Sidlerstrasse 5, 3102 Bern, Switzerland
[c] University of Liverpool, Department of Physics, L69 7ZE Liverpool, UK
[d] Technische Universität München, Lehrstuhl für Nukleartechnick, Boltzmannstrasse 15, 85748 Garching, Germany

ARTICLE INFO

Article history:
Received 16 April 2014
Received in revised form
11 June 2014
Accepted 11 June 2014
Available online 19 June 2014

Keywords:
Hadron beam
Foil activation
Calibration
FLUKA
Recoil nuclei
Secondary reactions

ABSTRACT

The well-known foil activation technique was used to calibrate an ionisation chamber employed for the on-line beam monitoring of a 120 GeV c^{-1} mixed proton/pion beam at CERN. Two monitoring reactions were employed: the standard $^{27}Al(p,3pn)^{24}Na$ and the alternative $^{nat}Cu(p,x)^{24}Na$. The parameters on which the technique critically depends and the adopted solutions are thoroughly analysed are the cross-section, the contribution of the competing reactions to the induced activity and the recoil nuclei effect. The experimental results are compared with FLUKA Monte Carlo simulations and with past results obtained with various calibration techniques. The comparison confirms that both reactions can be effectively employed. The $^{nat}Cu(p,x)^{24}Na$ reaction shows advantages because its cross-section is known at very high energies with a low uncertainty and the production of ^{24}Na is not affected by competing low energy neutron-induced reactions. The contribution of the competing reactions in the case of the $^{27}Al(p,3pn)^{24}Na$ reaction has been estimated to be 4.3%/100 mg cm^{-2}, whereas the effect of recoil nuclei is negligible.

1. Introduction

The intensity of high energy proton beams is monitored *via* measurements of the beam current, which can be performed *via* absolute measurement or indirect techniques [1,2]. Different devices can be employed: beam current transformers [3,4], Faraday cups [1,5] or particle detectors such as scintillators [6,7], ICs [8,9] and secondary electron emission monitors [10,11]. Beam current transformers measure the magnetic field induced by the passage of the particles, Faraday cups measure the beam electrical charge, while particle detectors measure the energy lost by particles in matter. Each technique shows some limitations: beam current transformers works only at high beam currents and are usually employed for pulsed beams; conventional Faraday cups provide extremely accurate measurements but are destructive and show peak power issues; scintillators are not radiation hard and show saturation effects above a certain threshold; ICs produce very low outputs; secondary electron emission monitors can usually be employed for intensities of at least few hundred pA, provided that the output signal is properly amplified, e.g. *via* a micro-channel plate, and show some drawbacks, such as the surface effect [12].

In the secondary beam areas of CERN SPS[1] the beam monitoring is commonly carried out *via* ICs. The high energy beams are characterised by a current varying between a few fA and tens of pA. These currents are too low to allow using beam current transformers and secondary electron emission monitors, whereas scintillators are used only in the lower part of the intensity range to avoid saturation, and Faraday cups cannot be used for on-line monitoring. Therefore ICs remain one of the best solutions, coupled with a low noise electronics designed to deal with the very low currents produced during the beam extraction from the SPS, from now on referred as beam "spill". A specificity of CERN secondary beam areas is that the beams are usually mixed particles, e.g. protons, pions and kaons for positive polarity. The relative percentages depend on the beam energy [13].

This paper discusses the foil activation technique for the calibration of ICs employed for monitoring high energy hadron beams. The focus is on the specific conditions of mixed high energy beams, but the conclusions are obviously valid for a beam composed of a single particle type. First, the activation of hyper-pure aluminium foils *via* the well-known $^{27}Al(p,3pn)^{24}Na$ reaction is discussed, focusing the attention on the different parameters on which the activation process critically depends and for which data in the literature are not always consistent. Then the alternative $^{nat}Cu(p,x)^{24}Na$ reaction is investigated, highlighting the features

* Corresponding author at: CERN, 1211 Geneva 23, Switzerland.
Tel.: +41 227662432; fax: +41 227667645.
E-mail address: giacomo.paolo.manessi@cern.ch (G.P. Manessi).

[1] IC=Ionisation chamber, SPS=Super proton synchrotron.

http://dx.doi.org/10.1016/j.nima.2014.06.045
0168-9002/

that makes it an ideal reaction for beam monitoring and its main advantages as compared to the ^{27}Al(p,3pn)^{24}Na. Finally the experimental results are compared with FLUKA [14,15] Monte Carlo simulations and with past results obtained *via* various other calibration techniques.

2. The foil activation technique

Foil activation is a well-established technique [16] for measuring the intensity of high energy proton beams. It is particularly convenient for the calibration of ICs used for on-line beam monitoring. One of its advantages is the accuracy that can be achieved if the cross-section of the reaction of interest is known with a small uncertainty. When the protons traverse the foil they generate spallation reactions A(p,x)B, where A is the stable isotope of which the foil is constituted, B is the radioisotope produced in the foil by the spallation reaction, whose activity is determined *via* γ-spectrometry, x represents the reaction products (one or more particles, depending on the reaction) escaping the foil. An ideal monitor reaction should show the following properties:

- Cross-section known with good accuracy.
- Half-life of the radioisotope produced in the foil longer than the irradiation time, but not too long in order to obtain a detectable activity.
- γ-Line(s) of the radioisotope produced in the foil easily detectable and distinguishable by γ-spectrometry.
- Negligible contribution to the production of the radionuclide of interest by secondary particles, such as neutrons and energetic secondary hadrons, formed by interaction of the proton beam in the target.

Unfortunately none of the commonly used reactions satisfy all of these requirements and one has to find a compromise. The bases of the activation theory are briefly recalled in Section 2.1. and the two monitor reactions employed in this study are discussed in Sections 2.2. and 2.3. The discussion will refer for simplicity to a proton beam, but the evaluations are valid for a generic hadron beam.

2.1. Theory

If $A(t)$ (Bq) is the activity induced in the foil, t_{IRR} and t_{WAIT} (s) are the irradiation time and waiting time, i.e. the time elapsed from the end of the irradiation until the foil is counted, N_x is the foil surface atomic density (cm^{-2}), σ is the production cross-section of the selected radioisotope (cm^2), the particle flux ϕ' (number of particles per second traversing the foil) can be obtained as (see Appendix)

$$\phi' = \frac{A(t)}{N_x \sigma (1 - e^{-\lambda t_{IRR}}) e^{-\lambda t_{WAIT}}}. \quad (1)$$

$A(t)$ is measured by γ-spectrometry, while t_{WAIT} and t_{IRR} must be recorded. In the present experiment t_{WAIT} was recorded manually while t_{IRR} was obtained from the log-file of the acquisition system.

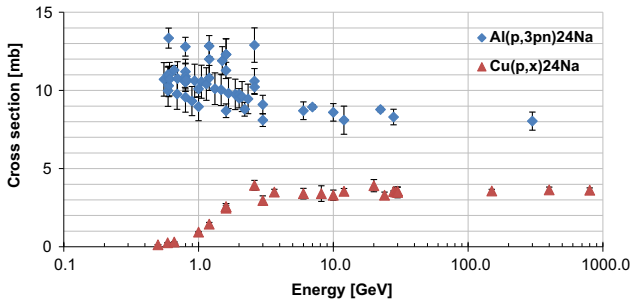

Fig. 1. Cross-section data available in the literature for the ^{27}Al(p,3pn)^{24}Na and the ^{nat}Cu(p,x)^{24}Na reactions for energies higher than 0.5 GeV [17].

2.2. The ^{27}Al(p,3pn)^{24}Na reaction

The ^{27}Al(p,3pn)^{24}Na reaction is one of the most extensively used beam monitor reactions [16]. Its main advantages are

- The short half-life of ^{24}Na (~15 h) results in a high specific activity so a relatively short irradiation time is adequate to obtain a reasonable activity to be determined by γ-spectrometry.
- ^{24}Na decays by β^- emission producing two γ-rays of energies 2.754 MeV and 1.369 MeV (branching ratios: 99.94% and 100%, respectively), whose peaks can be easily identified by γ-spectrometry.
- The ^{27}Al(p,3pn)^{24}Na cross-section is known with good accuracy in a wide energy range. Fig. 1 plots the available cross-section data for energies higher than 0.5 GeV. The 300 GeV value comes from indirect measurements [18].
- Hyperpure ^{27}Al foils are readily available.

To obtain an accurate determination of the particle flux, as derived from expression (1), one must take into account several parameters on which the reaction critically depends:

- The cross-section value at the energy of interest.
- The importance of the competing ^{27}Al(n,α)^{24}Na reaction, as well as of the reactions induced by energetic secondary hadrons produced in the foils, in the determination of the total induced activity.
- The recoil of some of the nuclei produced in the spallation process that can leave the foil in the same direction of the primary beam (see Fig. 2).

A first problem arises in the determination of the cross-section to be employed in case of a mixed proton/pion beam. Whilst for the proton-induced spallation reaction the cross-section data are available, for pion-induced reactions there are no published data. The value of the pion-induced cross-section can be indirectly determined using the FLUKA code. Even if FLUKA cannot be used to derive the absolute value of the cross-sections at very high energies with the required accuracy, it is much more reliable in the determination of the ratio of the cross-sections of reactions induced by different particles at the same energy on the same target. One can therefore calculate the ratio between the cross-section of pion- and proton-induced reactions and then derive the absolute value of the pion-induced one. The cross-section ratio can be obtained by running the nuclear interaction models of FLUKA in interaction only mode, accounting for both absorption and quasi-elastic reactions. The output file provides the cross-section for each isotope produced in the interaction between the primaries and the target. By running two simulations, for protons and for pions, one obtains the ratio between the pion- and the proton-induced cross-sections for the reaction of interest. Since the value of the proton-induced spallation cross-section of interest is known from the literature, one can derive the pion-induced cross-section and thus obtain the effective cross-section for the mixed beam.

The importance of the reactions induced by neutrons and energetic secondary hadrons in the production of ^{24}Na is discussed in Section 4.1.1. This effect has been evaluated *a posteriori* by analysing the induced activities of all the exposed foils.

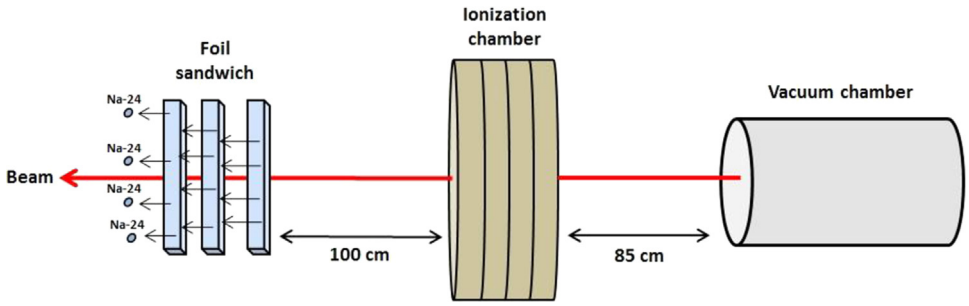

Fig. 2. Foil activation experiment set-up (not to scale).

Table 1
Specifications of the foils used in the activation experiments.

99.999% Al foils (ρ_{Al}=2.71 g/cm^3, M_{Al}=27 g/mol)			
Foil dimensions [mm^2]	50 × 50	50 × 50	50 × 50
Foil thickness X_{Al} [mm]	0.50 ± 0.05	1.0 ± 0.1	2.0 ± 0.2
Mass thickness [mg cm^{-2}]	135	270	540
Atomic density N_x [cm^2]	3.0222 × 10^{21}	6.0445 × 10^{21}	1.2089 × 10^{22}
Impurities [ppm]	Mg 1.2, Si 0.8, Cu 0.3, Fe 0.3		
99.99% Cu foils (ρ_{Cu}=8.92 g cm^{-3}, M_{Cu}=63.546 g mol^{-1})			
Foil dimensions [mm^2]	50 × 50	50 × 50	50 × 50
Foil thickness X_{Cu} [mm]	0.125 ± 0.001	0.250 ± 0.003	0.500 ± 0.005
Mass thickness [mg cm^{-2}]	111.5	223	446
Atomic density N_x [cm^2]	1.0567 × 10^{21}	2.1133 × 10^{21}	4.2266 × 10^{21}
Impurities [ppm]	Ag 70, Fe 2, Ni 2, Pb 2, Si 2, Al 1, Bi 1, Ca 1, Mg 1, Sn 1, Mn < 1, Na < 1,Cr < 1		

The foils were irradiated in sandwiches of three to take into account the recoil of some of the nuclei produced in the spallation process that can leave the foil in the same direction of the primary beam due to the so-called Lorentz boost [19]. In order to maintain the equilibrium between the loss of recoil nuclei knocked out of the foil and the gain of nuclei knocked into the foil from upstream material, only the central one must be considered for data analysis, whereas the upstream and the downstream ones act as catchers. These catchers, having the same thickness of the central foil, are thick enough to capture all the knocked on or knocked back products; this is because the foil is thicker than the projected range of the recoil nuclei in aluminium and copper. The importance of this effect is quantified in Section 4.1.2.

2.3. The ^{nat}Cu(p,x)^{24}Na reaction

The ^{nat}Cu(p,x)^{24}Na reaction is a promising alternative reaction for beam monitoring, as it shows two advantages when compared to ^{27}Al(p,3pn)^{24}Na:

- The cross-section, even if it is lower than that of ^{27}Al (p,3pn)^{24}Na, is known with better accuracy at high energies. Fig. 1 plots the available cross-section data for energies higher than 0.5 GeV. At very high energies (30, 150, 400 and 800 GeV) Baker et al. [20] found an energy-independent cross-section value of 3.59 ± 0.14 mb.
- ^{24}Na is produced only in deep spallation reactions induced by high energy hadrons, while the secondary neutrons produce mostly isotopes close to the original target mass.

The following two parameters play an important role in the determination of the particle flux:

- The value of the reaction cross-section at the energy of interest.
- The recoiling nuclei as discussed above.

In case of mixed proton/pion beams the same procedure described in Section 2.2. can be followed to obtain the effective beam cross-section. Values of proton-induced reaction cross-sections are widely available in the literature. As for the ^{27}Al foils, the ^{nat}Cu foils were exposed in sandwiches to compensate for the recoil effect.

3. Experiment

3.1. Experimental set-up

The foil activation technique was employed to calibrate the IC used for beam monitoring at the CERN-EU high-energy Reference Field (CERF) facility [21] at CERN. A positive hadron beam (61% pions, 35% protons and 4% kaons [13]) with momentum of 120 GeV c^{-1} is stopped in a copper target. The beam is delivered to the facility with a typical intensity in the range 10^6–10^8 particles per SPS spill. The beam extraction time is presently about 10 s over an SPS cycle of about 45 s.

The beam monitoring is provided by an air-filled, parallel-plate, transmission type IC placed in the beam a few metres upstream of the target. The IC has a diameter of 185 mm and consists of five parallel electrode plates made of Mylar with 17 mm inter-plate spacing. The central plate is the collector and the ones on either side are the polarity electrodes, whereas the external plates reduce the leakage of extraneous charge to the collecting electrodes. The polarisation voltage on these plates is supplied by an external battery. The beam traverses 34 mm of air at atmospheric pressure in the sensitive part of the chamber. The output signal is fed into a charge digitizer, which produces one signal, from now on called "count", every time a fixed amount of charge c is collected on the plates (c=8.403 × 10^{-13} C count^{-1}, determined experimentally [22]). These counts are acquired by a National Instrument USB 6342 DAQ connected to a desktop computer. The data are saved on

a log-file that records the differential and integrated IC readings, expressed in counts, every second.

Hyper-pure ^{27}Al and ^{nat}Cu foils from Goodfellow [23] were used, whose specifications are given in Table 1.

The foils were fixed on a Plexiglas frame mounted on both ends of a hollow aluminium tube of the same dimensions of the target normally employed at CERF (Fig. 2), placed downstream of the IC. The beam size was smaller than the foil dimensions so that all particles traversing the IC hit the foils. To evaluate the contribution of scattered radiation to the foil activation, in one of the experiments an additional foil was exposed out of beam.

3.2. Results

The spectrometry measurements were performed with a very low background XtRa (Extended Range) coaxial germanium detector by Canberra (GX4020 model) with a resolution of 2.0 keV (FWHM) at 1.33 MeV and relative efficiency $\geq$40%. The data acquisition and analysis was carried out by using the Genie-2000 and the PROcount-2000 software, which include a set of spectrum analysis algorithms and provide nuclide identification, interference correction, weighted mean activity, background subtraction and efficiency correction. The software takes into account geometrical effects, self-absorption in the sample and decay of the isotope during the spectrometry measurement. The results are given in Table 2. Where available, the activity of the upstream and downstream foils is given. The value used in expression (1) was the activity of the central foil, except for measurement 1 where, due to the high uncertainties, an average of the central and downstream foil activities was employed. Due to poor statistics and problems in the peak identification during the γ-spectrometry of the ^{nat}Cu 0.250 mm foil, the data of this measurement could not be exploited. The foil exposed out of beam did not show any significant induced activity for both materials, confirming that the contribution of the scattered radiation to the overall activity is negligible.

To obtain the IC calibration factor one needs to know the parameters in expression (1). To improve the accuracy of the calculation, the irradiation time was subdivided in one-second irradiation periods, thanks to the fact that the beam intensity was recorded every second in the acquisition log-files. The total activity was obtained as the sum of the partial activities induced by each one-second irradiation, by taking into account the decay of ^{24}Na occurring from the end of each one-second irradiation until the arrival in the spectrometry laboratory, about 30 min after the end of the irradiation. Therefore the beam-on/beam-off periods, i.e. spill time over the total SPS cycle (10 s and 45 s, respectively), were exactly taken into account and fluctuations in the beam intensity during the spill were also properly considered. The values of t_{IRR}, t_{WAIT} and ϕ' were then derived from the IC acquisition log-files, where all the quantities are registered every second. The surface atomic densities N_x are given in Table 1 for each foil. The beam effective cross-section was calculated as follows. For the ^{27}Al(p,3pn)^{24}Na reaction the proton-induced cross-section at 120 GeV c^{-1} was assumed equal to the one calculated by Cumming [16] at 28 GeV c^{-1}, i.e. 8.3 ± 0.5 mb. The pion/proton cross-section ratio was obtained by the FLUKA interaction models as described in Section 2.2., which gave 0.764 ± 0.011. The uncertainty is the statistical uncertainty of the Monte Carlo simulations. The pion-induced cross-section is then 6.3 ± 0.4 mb. The beam effective cross-section (63.5% pions and 36.5% protons: the kaon fraction, which accounts for only 4%, was re-distributed on the other two components according to their respective weight) is 7.1 ± 0.4 mb. For the ^{nat}Cu(p,x)^{24}Na reaction the proton-induced cross-section at 120 GeV c^{-1} was assumed equal to the one calculated by Baker et al. [20] at 30, 150, 400 and 800 GeV, i.e. 3.59 ± 0.14 mb. The pion/proton cross-section was found to be equal to 0.726 ± 0.016. The pion-induced cross-section is then 2.61 ± 0.12 mb and the beam effective cross-section is 2.93 ± 0.13 mb.

From expression (1) one can derive the value of the particle flux ϕ' and consequently the value of the raw calibration factors (before correction) for each experiment (see Table 3), where the uncertainties derive from the uncertainties on the activity, on the foil thickness (1%) and on the cross-section (5.6% and 4.4% for ^{27}Al(p,3pn)^{24}Na and ^{nat}Cu(p,x)^{24}Na, respectively). The uncertainty on the beam composition, which did not vary during the experiment, is not taken into account since it is below 2% [13].

The calibration factors from the aluminium activation need to be corrected for the contribution of the competing reactions to the overall activity. To take into account this contribution, which is proportional to the thickness of the foil, one has to extrapolate the calibration factor to zero thickness. Fig. 3 plots the calibration factors calculated from the different measurements with the corresponding linear fit. The extrapolated value is 22,249 ± 2100 particles count^{-1}, where the uncertainty is calculated *via* the reduced chi-square method. This correction is not needed for the values obtained from the copper activation, since the secondary neutrons do not produce ^{24}Na but mostly isotopes close to the original target mass. For the two measurements performed with Cu samples we can assume that, being these two results compatible within their range of uncertainties, the competing reactions induced by energetic secondary hadrons are of little importance. However, this will have to be verified in future measurements. The best estimation for the calibration factor, obtained *via* the weighted average method, is 22,293 ± 1462 particles count^{-1}.

All the results given above are based on the following assumptions:

- The ^{27}Al and ^{nat}Cu atoms are homogeneously distributed in the exposed foils. This is guaranteed by the supplier.

Table 2
Results of the foil activation experiment (uncertainties quoted at 1σ).

Al foils				
Measurement	1	2	3	4
Thickness [mm]	2.0	2.0	1.0	0.50
Irradiation time [s]	31,200	31,371	58,223	31,371
Integrated fluence [IC counts]	2×10^6	2.3×10^6	3.8×10^6	2.3×10^6
Upstream foil activity [Bq]	45.8 ± 2.2	n.a.	34.5 ± 1.9	n.a.
Central foil activity [Bq]	52.7 ± 5.4	56.8 ± 2.3	37.1 ± 1.9	12.3 ± 0.6
Downstream foil activity [Bq]	47.1 ± 1.6	n.a.	n.a.	n.a.

Cu foils			
Measurement	5	6	7
Thickness [mm]	0.500	0.250	0.125
Irradiation time [s]	54,831	54,831	54,831
Integrated fluence [IC counts]	3.3×10^6	3.3×10^6	3.3×10^6
Central foil activity [Bq]	8.4 ± 0.6	n.a.	2.3 ± 0.3

n.a.=not available.

Table 3
Raw calibration factors (before correction) as calculated from expression (1).

Measurement	Foil thickness (mm)	Raw calibration factor (before correction) [particles count^{-1}]
1	2.0 (Al)	27,736 ± 1682
2	2.0 (Al)	27,014 ± 1894
3	1.0 (Al)	25,040 ± 1923
4	0.50 (Al)	23,399 ± 1759
5	0.500 (Cu)	21,707 ± 1762
6	0.250 (Cu)	–
7	0.125 (Cu)	23,587 ± 2620

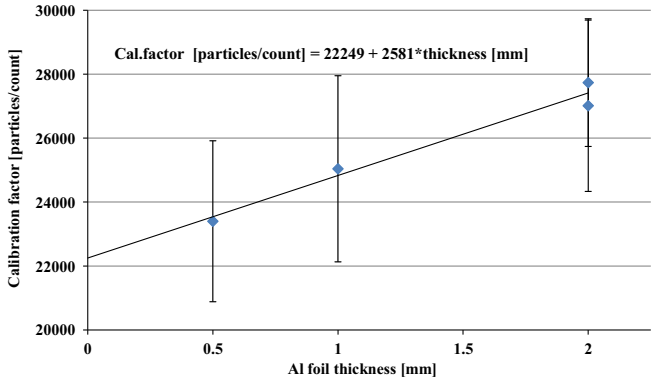

Fig. 3. Calibration factors calculated *via* the activation of the aluminium foils and linear fit to the data.

- The effect of the impurities present in the foils on the induced activity is negligible. This has been verified *via* FLUKA simulations in which the impurities declared by the supplier have been included in the foils. The difference in the activity by adding the impurities is less than 1%.
- The self-absorption of γ-rays in the activated foils is negligible. This has been verified by taking into account the most conservative case, i.e. the attenuation of the photons emitted by ^{24}Na in 2 mm of ^{27}Al and 0.5 mm of ^{nat}Cu. Since the mass attenuation coefficients are 3.54×10^{-2} cm^2 g^{-1} and 3.59 cm^2 g^{-1} [24], respectively, the maximum attenuation that the γ-rays can undergo before being detected by the spectrometer is less than 2%. This small effect is taken into account by the spectrometry software.

4. Discussion

The values of the calibration factor as derived *via* the activation of the aluminium and the copper foils are coherent within their range of uncertainties. These results can be compared with the calibration factor obtained *via* direct FLUKA simulations of the IC. The calibration factor can be derived *via* the knowledge of the expected charge q collected on the plates of the IC per primary particle:

$$q = E_{dep}\frac{e}{W_{AIR}} \tag{2}$$

where E_{dep} is the energy deposited by a primary particle in the sensitive volume of the IC, e is the electron charge (1.609×10^{-19} C) and W_{AIR} ($34.23\pm0.4\%$ eV [25]) is the average energy released by the primaries to produce a single ion pair in air. The energy deposited by 120 GeV c^{-1} protons, pions and kaons in the air volume of the IC ($p=0.963$ atm, $\rho=1.12\times10^{-3}$ g cm^{-3}) was assessed with FLUKA. The computed deposited energy accounts for the energy transported away by the delta rays that escape from the volume, and for the energy lost in the sensitive volume by the particle through nuclear reactions. The simulated fluence of all the particles produced by the beam in the experiment set-up is shown in Fig. 4: the beam is coming from the vacuum chamber (in grey) on the right, passes through the IC (in brown) and then hits the foil sandwich.

The results give an energy deposition value of 7.92 keV for protons, 8.15 keV for pions and 7.94 keV for kaons (with 1% uncertainty). Taking into account the beam composition, the weighted energy deposition is 8.06 keV. The expected charge deposited in the IC per beam particle is then 3.79×10^{-17} C. From the sensitivity factor of the IC charge digitizer one obtains the value of the calibration factor, i.e. the number of primaries needed to obtain one pulse from the charge digitizer: $c/q=22{,}172\pm789$ particles count^{-1}. The uncertainty is given by the uncertainty on W_{AIR} (0.4% systematic) and on E_{dep}, whose uncertainty is the sum of two components, the one derived from FLUKA simulations (1% statistical) and the one derived from the knowledge of the active length of the IC (3%, i.e. 1 mm over 34 mm, statistical). It should also be mentioned that there is also a systematic uncertainty on the FLUKA results, of the order of a few per cent for the part due to ionisation and of about 10% for the part due to nuclear interactions, which is not included in the uncertainties of the present result.

The calibration factor estimated *via* the FLUKA simulations is in agreement with the value determined experimentally (see Table 4). The present results are also in good agreement with past experimental results obtained with different calibration techniques: production of ^{18}F in Al foils ($23{,}000\pm2300$ particles count^{-1} [26]) and ^{11}C in ^{12}C foils ($23{,}400\pm1400$ particles count^{-1} [27]), and coincidence of scintillators ($22{,}116\pm92$ particles count^{-1} [28]).

4.1. ^{27}Al(p,3px)^{24}Na reaction

The activation of aluminium foils proved to be a reliable technique for the determination of the intensity of high energy hadron beams and the calibration of an IC. However, attention must be paid to the factors that could severely affect the experimental results. The cross-section value has been discussed in Section 2.2. This section describes *a posteriori* the effects of the competing reactions and of the recoil nuclei escaping the foil, based on the present experimental results.

4.1.1. Competing reactions

Two competing mechanisms lead to the production of ^{24}Na: the ^{27}Al(n,α)^{24}Na and the reactions induced by energetic secondary hadrons. The ^{27}Al(n,α)^{24}Na reaction has a threshold of 5.5 MeV and a cross-section rising to 120 mb at 14 MeV [29]. Data in the literature are contradictory about the importance of this effect. Some authors showed it has little importance: Stehney [30] measured a contribution of less than 1% per 200 mg cm^{-2} foil thickness, while Cumming et al. [31] proposed a value of 0.25% per 100 mg cm^{-2}. Other authors estimated a bigger importance: Brandt et al. [32] reported that this effect has an influence in the order of $1.1\pm0.5\%$ per 100 mg cm^{-2}, while Grover [33] showed a strong dependence on foil thickness, about 3.3% per 100 mg cm^{-2}. All these estimates refer to protons; no data are available for different particles. The contribution of the competing reactions has here been determined by analysing the results obtained from the present experiment. It is worth noting that this contribution may also depend on the materials present upstream and downstream of the target as well as on the characteristics of the resulting neutron "halo".

One can express the calibration factor as the sum of two terms: the first is due to the activity induced by the primary particles, the second to the activity induced by the secondary particles, neutrons and high energy hadrons, which is proportional to the foil mass thickness and to a coefficient k, expressed in per cent per 100 mg cm^{-2}:

$$C_x = C_{prim} + kC_{prim}x \tag{3}$$

where C_x is the calibration factor obtained for a foil of mass thickness x and C_{prim} is the calibration factor extrapolated to zero thickness. The constant k here refers to the partial activity due to the primary particles, whereas in other papers the contribution refers to the total activity. This choice was done to make expression (3) more consistent, even if the numerical difference is nevertheless of little importance. One can derive the value of the constant k from the linear fit in Fig. 3: $C_{prim}=22{,}249$ particles count^{-1}, $kC_{prim}=2581$ particles count^{-1} mm^{-1}. By normalising the constant to the foil mass thickness (1 mm = 271 mg cm^{-2}, see Table 1) one then

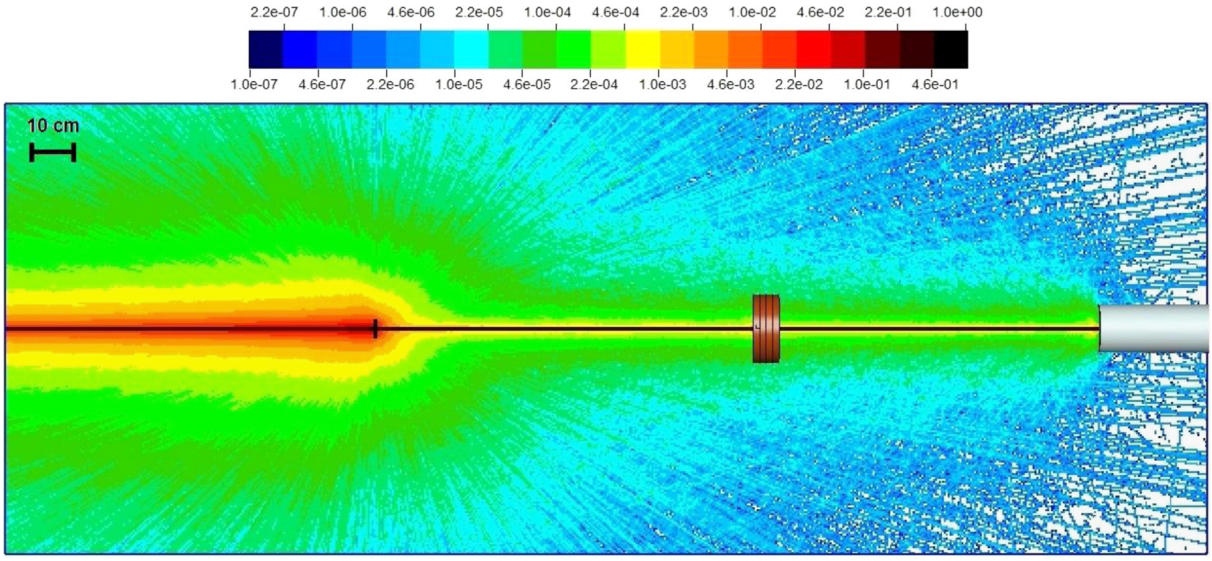

Fig. 4. Fluence of all particles (electron, kaons, neutrons, photons, protons and pions) produced by the beam in the experimental set-up (the legend is given in cm^{-2} per primary), plotted with SimpleGeo [34].

Table 4
IC calibration factor as obtained from the activation experiments and *via* FLUKA simulations.

Technique	IC calibration factor [particles $count^{-1}$]
Activation of ^{27}Al foils	$22{,}249 \pm 2100$
Activation of ^{nat}Cu foils	$22{,}293 \pm 1493$
FLUKA simulations	$22{,}172 \pm 789$

obtains $k = 0.116\ mm^{-1} = 4.3\%/100\ mg\ cm^{-2}$, close to the data of Grover for protons [33]. It must be noted that the value obtained by Grover refers to the $^{27}Al(n,\alpha)^{24}Na$ reaction only, whereas here the two contributions cannot be evaluated separately.

4.1.2. Recoil nuclei effect

To take into account the recoil nuclei effect only the activity of the central foil of the sandwich was employed in expression (1), except for measurement 1. The loss of nuclei knocked out of the foil is in fact not compensated in the case of the upstream one. To verify the importance of the effect, for some measurements several analyses were carried out (see Table 2). However all the activity values are compatible within 2σ. This shows that the importance of this effect is limited. This is confirmed by the FLUKA interaction models, which give a mean energy of the recoil ^{24}Na nuclei of about 2 MeV. This corresponds to a projected range of 2 μm in the Al target, i.e. only the nuclei produced in the last layer (a few microns) of the foil escape in the beam direction. This fraction corresponds to a maximum of about 0.4% on the overall activity for the 0.5 mm sandwich.

4.2. $^{nat}Cu(p,x)^{24}Na$

The IC calibration performed *via* the activation of copper foils showed results consistent with those obtained by the better known activation of aluminium foils. Moreover, due to the higher accuracy with which the cross-section of the $^{nat}Cu(p,x)^{24}Na$ reaction is known, the final uncertainty is lower. The validity of this alternative reaction is also confirmed by the agreement with the results obtained from the FLUKA simulations. The $^{nat}Cu(p,x)^{24}Na$ reaction has the advantage that there are no competing neutron-induced reactions producing ^{24}Na and that the contribution from energetic secondary hadrons is negligible. The importance of the recoil nuclei effect is limited also in this case, since the FLUKA interaction models give a mean energy of the recoil ^{24}Na nuclei of 11 MeV, which corresponds to a projected range of 3 μm in the Cu target, i.e. about 2.5% on the overall activity for the 0.125 mm sandwich.

5. Conclusions

Both monitoring reactions employed in the present activation experiment showed to be reliable. This is confirmed by the excellent agreement of the value of the IC calibration factor derived from the measurements with the two materials with the value obtained from the FLUKA simulations and with results of past calibrations carried out with different techniques. The $^{nat}Cu(p,x)^{24}Na$ reaction shows several advantages if compared to $^{27}Al(p,3px)^{24}Na$: competing reactions play a little role and the final uncertainty on the result is lower because of the higher accuracy with which the absolute cross-section is known at very high energies. However, since the cross-section is lower than that of the $^{27}Al(p,3px)^{24}Na$ reaction, a longer irradiation time is necessary in order to decrease the statistical uncertainty of the γ-spectrometry measurements. The effect of the competing reactions on the overall activity in the case of the activation of aluminium foils has been derived for the mixed proton/pion beam used in this experiment, i.e. $4.3\%/100\ mg\ cm^{-2}$. Similarly the effect of loss of recoil nuclei knocked out of the foil showed to be of very little importance. For future experiments, the geometry could be improved by employing catcher foils with a lower thickness, comparable to the projected range of the recoil nuclei in that material, in order to reduce the production of secondary particles. On the other hand, thicker central foils could significantly reduce the statistical uncertainty by increasing the induced activity.

Acknowledgements

The authors wish to thank Matteo Magistris (CERN) for providing access to the γ-spectrometry laboratory, Carsten Welsch (university of Liverpool), Yann Donjoux and Francesco Cerutti (CERN) for useful discussions, Nicolas Sabbi, Nicolas Riggaz and

Biagio Zaffora (CERN) for performing the γ-spectrometry measurements and Clizia Severino (CERN) for assisting with some of the measurements.

Appendix A

The production of a radionuclide of interest at a time t is expressed by the well-known formula:

$$n(t) = \frac{N\sigma\phi}{\lambda}(1-e^{-\lambda t_{IRR}})e^{-\lambda t_{WAIT}} \quad (A1)$$

where $n(t)$ is the number density of the atoms of the radionuclide of interest at time t (cm^{-3}), N is the number density of the target atoms (cm^{-3}, where $N=\rho N_{AV}/M$: ρ is the mass density in g cm^{-3}, N_{AV} is Avogadro's number 6.022×10^{23} mol^{-1}, M is the molar mass expressed in g mol^{-1}), σ is the production cross-section of the selected radioisotope (cm^2), λ is its decay constant (s^{-1}), ϕ is the particle flux density (cm^{-2} s^{-1}), t_{IRR} and t_{WAIT} (s) are the irradiation time and waiting time respectively. The specific activity induced in the target at time t is given by $a(t)=\lambda n(t)$:

$$a(t) = N\sigma\phi(1-e^{-\lambda t_{IRR}})e^{-\lambda t_{WAIT}} \quad (A2)$$

where $a(t)$ is expressed in Bq cm^{-3}. If L_1, L_2 are the transverse dimensions of the target and Δx its thickness the absolute activity $A(t)=a(t)L_1L_2\Delta x$ in Bq is equal to

$$A(t) = N\Delta x\sigma\phi L_1L_2(1-e^{-\lambda t_{IRR}})e^{-\lambda t_{WAIT}}. \quad (A3)$$

If $N_x=N\Delta x$ is the surface atomic density (cm^{-2}), the particle flux $\phi'=\phi L_1L_2$ (number of particles per second traversing the foil) is given by (expression (1) in Section 2.1)

$$\phi' = \frac{A(t)}{N_x\,\sigma\,(1-e^{-\lambda t_{IRR}})\,e^{-\lambda t_{WAIT}}}. \quad (A4)$$

References

[1] D. Yount, Nuclear Instruments and Methods 52 (1967) 1.
[2] P. Forck, Beam Current Measurements, Lecture Given at the Joint Universities Accelerator School (JUAS), Archamps, France, 2013. Available at: ⟨http://www-bd.gsi.de/conf/juas/current_trans.pdf⟩.
[3] H. Feist, M. Koep, H. Reich, Nuclear Instruments and Methods 97 (1971) 319.
[4] J. Belleman, D. Belohrad, L. Jensen, M. Krupa, A. Topaloudis, Proceedings of the 2nd International Beam Instrumentation Conference (IBIC), Oxford, 2013.
[5] J. Harasimowicz, C.P. Welsch, Proceedings of the 2010 Beam Instrumentation Workshop (BIW), Santa Fe, New Mexico, USA, 2010.
[6] L.L. Kanstein, R.E. Morgado, D.U. Norgren, R.W. Sorensen, Nuclear Instruments and Methods 118 (1974) 483.
[7] J.H. So, H.J. Kim, H. Kang, H. Park, S. Ryu, S.W. Jung, Journal of the Korean Physical Society 50 (2007) 1506.
[8] A.J. Metheringham, T.R. Willitts, Nuclear Instruments and Methods 15 (1962) 297.
[9] H.S. Kim, S.H. Park, Y.K. Kim, J.H. Ha, S.M. Kang, C.E. Chung, Journal of the Korean Physical Society 48 (2006) 213.
[10] B. Planskoy, Nuclear Instruments and Methods 24 (1963) 172.
[11] K. Bernier, G. de Rijk, G. Ferioli, E. Hatziangeli, A. Marchionni, V. Palladino, G.R. Stevenson, T. Tabarelli de Fatis, E. Tsesmelis, CERN Yellow Report 97-07, 1997.
[12] L. Badano, O. Ferrando, M. Caccia, C. Cappellini, V. Chmill, M. Jastrzab, K. Abbas, U. Holzwarth, P.N. Gibson, Proceedings of the 2007 European Workshop on Beam Diagnostics and Instrumentation for Particle Accelerators (DIPAC), Venice, Italy, 2007.
[13] H.W. Atherton, C. Bovet, N. Doble, G. Von Holtey, L. Piemontese, A. Placci, M. Placidi, D.E. Plane, M. Reinharz, E. Rossa, CERN Yellow Report 80-07, 1980.
[14] A. Ferrari, P.R. Sala, A. Fassò, J. Ranft, CERN-2005-10, INFN/TC_05/11, SLAC-R-773, 2005.
[15] G. Battistoni, S. Muraro, P.R. Sala, F. Cerutti, A. Ferrari, S. Roesler, A. Fassò, J. Ranft, in: M. Albrow, R. Raja (Eds.), Proceedings of the 2006 Hadronic Shower Simulation Workshop on AIP Conference, vol. 896, Fermilab, US, 2007, p. 31.
[16] J.B. Cumming, Annual Review of Nuclear Science 13 (1963) 261.
[17] Nuclear reaction database (EXFOR): ⟨http://cdfe.sinp.msu.ru/⟩, 2014.
[18] S.B. Kaufman, M.W. Weisfield, E.P. Steinberg, B.D. Wilkins, D.J. Henderson, Physical Review C 19 (1979) 962.
[19] D. Filges, F. Goldenbaum, Handbook of Spallation Research, Wiley-VCH, Weinheim, 2009.
[20] S.I. Baker, R.A. Allen, P. Yurista, Physical Review C 43 (1991) 2862.
[21] A. Mitaroff, M. Silari, Radiation Protection Dosimetry 102 (2002) 7.
[22] F.P. La Torre, G.P. Manessi, F. Pozzi, C.T. Severino, M. Silari, CERN-RP-2013-083-REPORTS-TN, 2014.
[23] GoodFellow, See Online Catalogue at ⟨http://www.goodfellow.com⟩, 2014.
[24] Korea Atomic Energy Research Institute (KAERI), Photon Cross-sections and Attenuation Coefficients, ⟨http://atom.kaeri.re.kr⟩, 2014.
[25] IAEA, Technical Report Series 398, 2000.
[26] M.C. Hopper, C. Raffnsoe, G.R. Stevenson, CERN/TIS/RP/TM/93-21, 1993.
[27] G.R. Stevenson, J.C. Liu, K. O'Brien, J. Williams, CERN/TIS/RP/TM/94-15, 1994.
[28] H. Vincke, S. Mayer, I. Efthymiopoulos, A. Fabich, D. Forkel-Wirth, M.J. Muller, C. Theis, CERN/SC/RP/TN/2004-090, 2004.
[29] J.P. Butler, D.C. Santry, Canadian Journal of Physics 41 (1963) 372.
[30] A.F. Stehney, Nuclear Instruments and Methods 59 (1968) 102.
[31] J.B. Cumming, J. Hudis, A.M. Poskanzer, S. Kaufman, Physical Review 128 (1962) 2392.
[32] R. Brandt, C. Gfeller, W. Stotzel-Riezler, Nuclear Instruments and Methods 62 (1968) 109.
[33] J.R. Grover, Physical Review 126 (1962) 1540.
[34] C. Theis, K.H. Buchegger, M. Brugger, D. Forkel-Wirth, S. Roesler, H. Vincke, Nuclear Instruments and Methods A 562 (2006) 827.